High pressure tuning of whispering gallery mode resonances in a neodymium-doped glass microsphere

L. L. Martin,[1,*] S. F. León-Luis,[1,2] C. Pérez-Rodríguez,[1] I. R. Martín,[1,2,3] U. R. Rodríguez-Mendoza,[1,2] and V. Lavín[1,2]

[1]*Departamento de Física Fundamental y Experimental, Electrónica y Sistemas, Universidad de La Laguna, 38200 San Cristóbal de La Laguna, Santa Cruz de Tenerife, Spain*
[2]*Malta Consolider Team, Universidad de La Laguna, 38204 San Cristóbal de La Laguna, Santa Cruz de Tenerife, Spain*
[3]*Instituto de Materiales y Nanotecnologia (IMN), Universidad de La Laguna, 38204 San Cristóbal de La Laguna, Santa Cruz de Tenerife, Spain*
**Corresponding author: lmartin@ull.es*

Received July 23, 2013; revised October 29, 2013; accepted October 31, 2013; posted October 31, 2013 (Doc. ID 194450); published November 20, 2013

The effects of pressure on the behavior of optical microspherical resonators, prepared from Nd^{3+} doped, barium titanium silicate glass, have been studied up to 5 GPa inside a diamond anvil cell using silicone oil as the hydrostatic transmission medium and ruby emission lines as the pressure gauge. The optical resonances, known as whispering gallery modes, were observed within the broad emission band of the Nd^{3+} ions, and the resonances were identified as a function of pressure. By means of simulations, it was found that the average wavelength position of both transverse electric and magnetic modes depended on the radius and refractive index of the sphere, but not on the refractive index of the pressure transmitting medium under the experimental conditions. This was used to define the average sensitivity of the resonant modes with the pressure. Therefore, a value of 6.5×10^{-4} GPa^{-1} has been obtained for this sensitivity, which is higher than the value for ruby, the most conventional pressure sensor.

OCIS codes: (280.4788) Optical sensing and sensors; (280.5475) Pressure measurement; (140.4780) Optical resonators.
http://dx.doi.org/10.1364/JOSAB.30.003254

1. INTRODUCTION

In the last several years, optical sensing devices and, especially, optical nano and microsensing devices have attracted much attention because of their advantages compared to traditional electric transducers in terms of properties such as electrical passiveness, greater sensitivity, freedom from electromagnetic interference, wide dynamic range, point and distributed configurations, and multiplexing capabilities [1]. Generally, in accordance with which property of the light beam changes when interacting with the optical sensors, devices can be classified into two groups: those for which the optical phase is affected (interferometers) and those in the other group that include devices based on the modulation of the intensity.

Recently, a new group of optical microsystems has been proposed as sensors in the interferometric category. They present morphology dependent resonances, known as whispering gallery modes (WGM) [2,3]. These sensors have a microstructure made of a transparent dielectric whose refractive index is higher than that of the surrounding medium in order to generate total internal reflection and to act as the resonant cavity. In addition, these optical microcavities have other applications such as in micron size lasers, add/drop filters for fiber communications, laser stabilization, and so forth.

Although the use of microresonators as temperature sensors is well studied [2,4], the behavior of these devices has not been investigated in the range of high pressures (several GPa). This is due to one common limitation of studies on nondoped microresonators, which is the need for a coupling device to observe the resonances on passive resonators. Therefore, its use is impossible inside the diamond cell that should be used in order to reach the GPa range; to avoid this difficulty, a noncoupling scheme proposed by the authors [5] was employed with optically active resonators.

The luminescent properties of optically active ions are useful in the employment of the microsphere as an optical remote sensor. The characteristic spectra of trivalent rare earth (RE^{3+})-doped glass microresonators consist of a series of sharp emission peaks, known as WGM resonances, whose intensities are modulated by the spontaneous emission of the RE^{3+} ions. These sharp emission peaks are due to the resonant cavity interaction with the spontaneous emission of the RE^{3+} ions inside of the microsphere. In order to describe the quality of the resonators, it is possible to introduce a dimensionless parameter that takes into account the storage time of the energy inside the resonator; this is the quality factor Q, and it is also related to the spectral width of the resonances.

On the other hand, a variety of effects can partially take out the light of the resonant path, thereby constituting losses in the cavity and diminishing the storage energy, and thus, the Q factor. Two of the most important loss mechanisms affecting our experiment are the absorption in glass and surface scattering.

The microspheres used in this study were fabricated from Nd^{3+}-doped barium titanium silicate (BTS) glass. This is glass that has been studied and is known to produce transparent glass-ceramics by conventional thermal treatment or by laser heating [6], with high nonlinear coefficients [7]. The Nd^{3+}-doped BTS microspheres also have shown laser emission [8]. In previous work, the possibility of using the Nd^{3+}-doped BTS glass microspheres as optical temperature sensors was studied [4]. The shifts of the peaks with the temperature were explained on the basis of the variation of the refractive index and on changes of the radius of the microsphere due to dilatations initiated by the effect of the temperature.

The scope of this work is to analyze the effects of pressure on the WGM generated in the BTS microspheres and to investigate the possibility of using them as optical pressure sensors.

2. THEORETICAL BACKGROUND

In order to establish a pressure gauge to study the effects of pressure on the microspheres, the average pressure inside of the chamber was calculated from the wavelength of the R_1 emission line of ruby using the Piermarini equation [9], i.e.,

$$P = \frac{A}{B}\left\{\left[1 + \left(\frac{\Delta\lambda}{\lambda_0}\right)\right]^B - 1\right\}, \tag{1}$$

where P is the pressure in GPa, λ_0 is the wavelength in nm of the R_1 line of ruby, $A = 1904$ and $B = 7.665$ for quasi-hydrostatic conditions [9], and $\Delta\lambda$ represents the shift of this line with pressure.

The position of the WGM resonant peaks in wavelength (nm) can be roughly obtained by a geometrical approximation from the following equation:

$$\lambda = \frac{2\pi n_{\text{eff}} R_S}{l}, \tag{2}$$

where n_{eff} is the effective refractive index of the sphere, R_S is the radius of the sphere, and l is the polar mode number that represents the number of wavelengths that fit into the resonator.

A more detailed description can be found in the article of Little *et al.* [10], in which the polarization of the resonant mode, transverse electric (TE) or transverse magnetic (TM), and the refractive index of the media surrounding the sphere are considered as follows:

$$\left(p \cdot \alpha_S + \frac{l}{R_S}\right) \cdot j_l(kn_S R_S) = k \cdot n_S \cdot j_{l+1}(kn_S R_S), \tag{3}$$

where

$$\alpha_S = \sqrt{\beta_l^2 + k^2 n_o^2}, \quad \beta_l = \frac{\sqrt{l(l+1)}}{R_S}, \quad k = \frac{2\pi}{\lambda},$$

and

$$p = \begin{cases} 1 & \text{TE modes} \\ n_r^2 & \text{TE modes; } n_r = n_s/n_o \end{cases}.$$

Here, n_s and n_o are the refractive index of the microsphere and the outer surrounding medium, respectively, and $j_l(kn_sR_s)$ is the spherical Bessel function. This equation can be asymptotically solved in terms of the zeros of the Airy function to facilitate the work on simulation with the Bessel functions [11]. The approximated solutions for the first radial order (the one observed in the experiments) is:

$$k = \frac{1}{n_o R_s}\left[\frac{l+1/2}{n_r} + \frac{\zeta_1}{n_r}\left(\frac{l+1/2}{2}\right)^{1/3} - \frac{p}{\sqrt{n_r^2 - 1}} + \frac{3\zeta_1^2}{20 n_r}\left(\frac{l+1/2}{2}\right)^{-1/3} + \ldots\right], \tag{4}$$

where the parameter ζ_l is the l-th zero of the Airy function and the other parameters are the same as those described above. This approximation is accurate enough [11] for the simulation of pressure-induced shifts in the wavelength of the WGM resonances on the basis of changes in the parameters involved: n_s, n_0, and R_s. These changes of the positions of the WGM can be characterized in terms of the sensitivity parameter (S), a common parameter regarding optical sensors, which can be expressed as follows, assuming no dependence of the external refractive index [2]:

$$S = \frac{\partial\lambda}{\lambda\partial P} = \frac{\partial n_S}{n_S \partial P} + \frac{\partial R_S}{R_S \partial P}. \tag{5}$$

Regarding the optical quality of the resonator Q, it is related to the temporal storage time of the cavity, and hence, to the spectral full width at half-maximum (FWHM) of the resonances λ. It can be described as [12]:

$$\frac{1}{Q} = \frac{1}{Q_R} + \frac{1}{Q_C} + \frac{1}{Q_S} + \frac{1}{Q_M} = \frac{\lambda}{\text{FWHM}(\lambda)}, \tag{6}$$

where Q_R represents radiative losses (negligible for $l \geq 50$ [12]); Q_C describes the losses due to coupling to an external device, not present in this experiment; Q_S characterizes the losses associated with surface scattering due to imperfections, scratches, or particles stuck to the surface; and Q_M takes into account the material losses due to absorption and scattering inside the microsphere. In fact, these last two factors are those that limit the quality factor in our resonators.

In addition, other processes can increase the observed spectral width of the resonances. For example, because of the existence of a small ellipticity on the microsphere, each single radius has a single narrow resonance, but the superposition of several narrow peaks produces a broad resultant. This reasoning is also found in a recent work [13], where the broadening effect is attributed in equivalent terms to the ellipticity pointed out here.

3. EXPERIMENTAL METHODS

The microspheres were produced from BTS glass with the composition of 40%BaO-20%TiO_2-40%SiO_2 and doped in excess with 1.5% Nd_2O_3 (in mol %). Commercial powders of ACS reagent grade (purity ≥99.99%) $BaCO_3$, TiO_2, SiO_2, and Nd_2O_3 were mixed and melted in a Platinum–Rhodium crucible at 1500°C for 1 h in an electric furnace. After that, the melt was poured between bronze plates following the melt-quenching method. The spherical shape of the microspheres can be made by different methods, which include polishing, chemical etching, and rapid quenching of liquid droplets. In this work, the microspheres were fabricated by the last method, described in detail by Elliot *et al.* [14], from the glass

mentioned above. The microspheres obtained ranged in diameter from 10 to 100 μm.

High pressure experiments were performed with a diamond anvil cell (DAC) [15] in a sample chamber (150 μm diameter) made from a pre-indented Inconel-750 gasket. The chamber was filled with silicone oil (Dow Corning 200 fluid, 50 cst.) as the pressure transmitting medium. The hydrostatic condition for this medium cannot be assured above 3 GPa [16].

A microscope objective was employed to focus a 532 nm diode-pumped solid-state (DPSS) laser in order to excite the Nd^{3+} ions, whose emission was partially coupled to the microsphere resonances. The fluorescent light emitted by the microsphere was collected using the same objective and focused into the entrance slit of a CCD spectrograph. As previously described [5], to obtain the highest contrast and best visualization of the resonances, it is important to keep the laser focused at the center of the sphere and to measure the luminescent resonances on the surface of the microsphere. A linear polarizer was located in the optical path (in the collimated area and before mirrors) with the aim of discriminating between the TE and TM modes. Because of the geometry of the experiment, the TM modes were obtained with the polarizer at 0° and the TE at 90°. As a result of the presence of the mirrors and the polarization response of the diffraction grating, the intensity of the TE and TM modes were not comparable and only the positions of the peak centroids were taken into account. In order to avoid erroneous readings on the peak shift of the WGM or the ruby line by small offsets of the spectrograph, the spectrum of a Neon lamp was measured after each spectrum in order to accurately correct the wavelength originated by small grating displacements, thus ensuring wavelength errors smaller than the resolution limit of the system.

In order to ensure the quality of the obtained data, the BTS microspheres were selected by a screening process and only the ones with the highest quality factors (i.e., sharpest resonances and no obvious scratches or defects) and best spatial homogeneity of the resonances (meaning negligible ellipticity) were inserted into the DAC.

One potential limitation of this study is the self-heating of the microsphere by laser irradiation [4], because this process can interfere with the shift produced by the pressure effect with a significant rate of 11 pm/K. Thus, in order to avoid laser heating of the BTS microsphere, the resonances were measured over a wide range of laser pump powers at various pressures; the wavelength shift was below our resolution limit (0.3 nm) up to 25 mW of incident laser power. To be conservative, the pump power employed was 5 mW to ensure that no thermal effects were caused by heating of the sphere up to 6 K.

4. RESULTS AND DISCUSSION

The spectra obtained from the Nd^{3+}-doped BTS microsphere at ambient pressure in air, before introduction into the DAC, are shown in Fig. 1. The two spectra were obtained by detecting the luminescence at the center (black line) and at the surface (red line) of the BTS microsphere. The first one shows the characteristic emission of the $^4F_{3/2} \rightarrow {}^4I_{9/2}$ multiplet of Nd^{3+} ions in the BTS glass, while the red line shows this emission modulated by the WGM resonances of the microsphere.

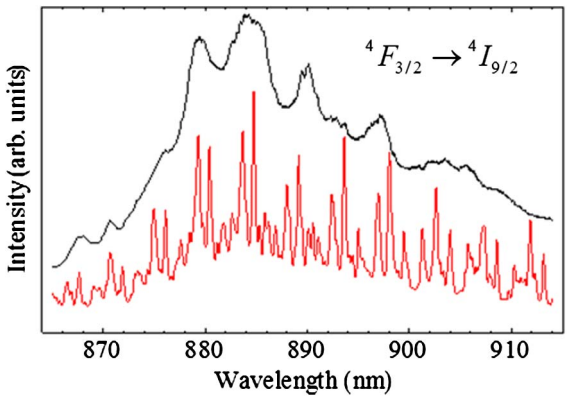

Fig. 1. Spectrum of a microsphere obtained at the center of the microsphere (in black), which shows the broad $^4F_{3/2} \rightarrow {}^4I_{9/2}$ band emission of Nd^{3+} ions in the BTS glass, and spectrum obtained at the air–microsphere boundary (in red), which shows the characteristic WGM pattern.

The advantage of using the spectra of the resonances in air is that the refractive index of the air is known and, therefore, only two parameters need to be fitted. From these spectra, and using values of $n_s = 1.71$ and $R_S = 20$ μm in Eq. (4), the polar mode l can be estimated by iterative change of the parameters and comparison with the position of the resonant peaks at ambient pressure in air (see Fig. 1). The found values were $l = 230$ for the TE modes and $l = 231$ for the TM modes for the peaks centered at 884 and 886 nm, respectively. These parameters n_S, R_S, and l are useful in the simulations, which will be explained later.

Figure 2 (left) shows the optical image of the microsphere inside the DAC, in which different ruby microcrystals at various positions inside the pressure chamber, denoted as R1–R5, are also visible. The R1 ruby has been employed as the pressure gauge for the high pressure experiments, since it is the closest one to the microsphere. The others were employed to sense the possible nonhydrostaticity of the pressure transmitting medium, the pressure gradient, and/or the pressure uncertainty inside the chamber by comparing the pressures between them. Figure 2 (right) represents an image of the microsphere excited by the 532 nm laser, where the laser was filtered-out in order to detect the spontaneous fluorescence of the Nd^{3+} ions in the microsphere.

The simulated dependence of the position of the TE and TM modes on the variation of the outer (silicone) and inner (BTS)

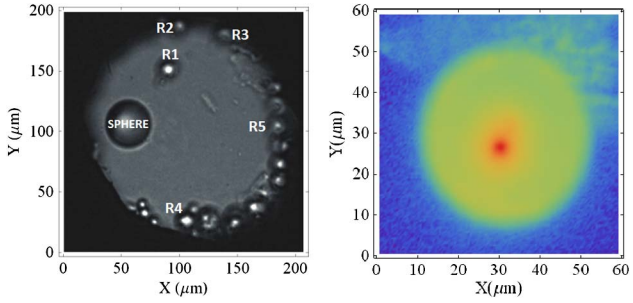

Fig. 2. Picture of the pressure chamber inside the diamond anvil cell at visible light (Left), in which the microsphere and the ruby chips (labeled R1–R5) employed as pressure gauges are clearly observed. Fluorescent image (false color) of a microsphere with a radius about 20 μm in air (Right), illuminated by a 532 nm laser and showing the Nd^{3+} luminescent emission between 880 and 900 nm.

refractive indexes and the radius of the microsphere with pressure was estimated from Eq. (4) using the parameters fitted in the previous step (n_S, R_S, and l). On the other hand, the value of the refractive index of the medium given by the fabricant is $n_0 = 1.30$ at 550 nm, but the value of $n_0 = 1.25$ at 890 nm achieved a better fitting to the positions of the resonances at the initial pressure, where the changes of the wavelength are attributed only to the change of the outer refractive index from air to the silicone oil.

These three parameters were varied considering the data found in the literature regarding the elastic coefficients of the BTS glass [17] and the photoelastic coefficient of a similar glass [18]. This was done in order to analyze the effect of the pressure on the parameters.

As shown in Fig. 3 (top), changing the radius of the sphere from 19.8 to 20.2 μm caused the resonant peak positions to suffer a red-shift of around 15 nm, while the TM–TE wavelength gap was nearly constant. The main effect of pressure is to reduce the volume of the microsphere; thus, it is expected that the radius will decrease when the pressure increases, thereby producing a net blue-shift of the resonance emission peaks.

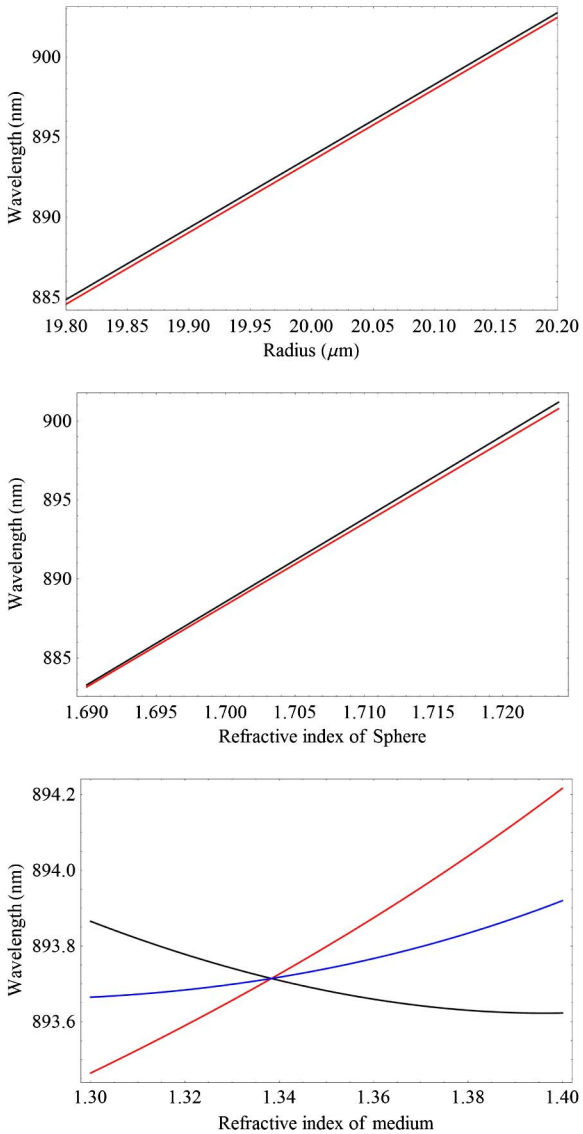

Fig. 3. Simulated positions of the resonances using Eq. (4) where the parameters are $n_s = 1.71$, $R_s = 20$ μm, and $n_o = 1.25$. The parameter of the x axis varies by 2% from the nominal value. (Top) Variation of the spheres radius. (Central) Variation of the refractive index of the sphere. (Bottom) Variation of the refractive index of the outer medium. Red line is the TE_{230}, black line is the TM_{231}, and blue line is the λ_{AVG} given by Eq. (7).

The effects of changing the refractive index of the sphere from 1.69 to 1.72 on the resonances are depicted in Fig. 3 (central). Also, there was a nearly linear red-shift when increasing the refractive index, although it was possible to appreciate a small difference between the wavelengths of the TM and TE modes that increased with the refractive index. As the pressure increases, the refractive index should increase, which means that the resonances would shift to longer wavelengths; thus, a red-shift is expected when the pressure is increased when considering only this effect.

If the refractive index of the pressure transmitting medium was increased from 1.30 to 1.4, as shown in Fig. 3 (bottom), the TE and TM resonances displayed opposite shifts, i.e., while the TE modes were red-shifted, the peaks of the TM modes were blue-shifted. As the movements were nearly symmetric, it is possible to compute the combined displacement of the two modes by:

$$\lambda_{AVG} = \frac{\lambda_{TE(l)} + \lambda_{TM(l+1)}}{2}. \tag{7}$$

It is worth noting that this result predicts that the average wavelength is nearly independent of the surrounding media and has a maximum deviation of around ±0.3 nm in the simulated range of the outer refractive index. This is quite interesting since it allows obtaining the pressure sensitivity parameter independently from the pressure transmitting medium employed, at least for some particular values of the outer and inner refractive index. Taking this fact into account in this study, the sensitivity given by Eq. (5) becomes independent of n_o, as was stated, and it is possible to introduce the λ_{AVG} in Eq. (5) in order to obtain an averaged sensitivity S_{AVG}.

Therefore, the radius and the refractive index of the microsphere affect the average position of the TE and TM resonances.

The experimental positions of the centroids of the TE and TM resonant peaks as a function of the rising pressure, from ambient conditions up to 5 GPa, are shown in Fig. 4. On the plot, it is possible to observe the net shift to blue of the

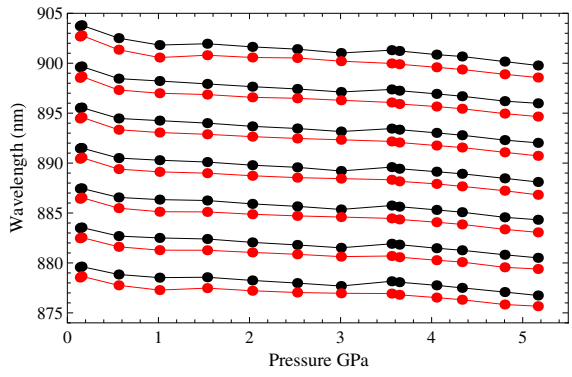

Fig. 4. Positions of the resonances at rising pressures. Black data correspond to the TM modes and red data to the TE modes.

resonances, which is not perfectly linear and contains some differences on the distance of the TE and TM modes.

The average wavelength position obtained using Eq. (7) can be observed in Fig. 5; the results show a clear shift to blue with a slope of around -0.58 nm GPa^{-1} and a zone of nonlinear behavior found at about 3.5 GPa that could correspond to a change in the outer medium. According to the previous simulations, the average wavelength was nearly independent of the surrounding medium and the blue-shift indicates that the change in the radius of the microsphere predominates over the change of its refractive index. However, as it will be justified below, both contributions are needed to explain the results shown in Fig. 5.

The displacement produced in the wavelength is completely reversible, and the position of the peaks returns to its initial value when the pressure is released to its initial value. Although the experimental limitations of our DAC do not allow for a smooth decrease of the pressure, some points of the round trip to 0 GPa were measured and added as red dots to Figs. 5 and 6, thereby proving that the changes in radius and refractive index were completely elastic.

Since the bulk modulus K of the BTS glass is known [17], it is possible to deduce the dependence of the radius of the sphere as a function of pressure, i.e.,

$$\frac{1}{R_S}\cdot\frac{\partial R_S}{\partial P} = -\frac{1}{3K} = -57\times 10^{-4}\ \text{GPa}^{-1}. \tag{8}$$

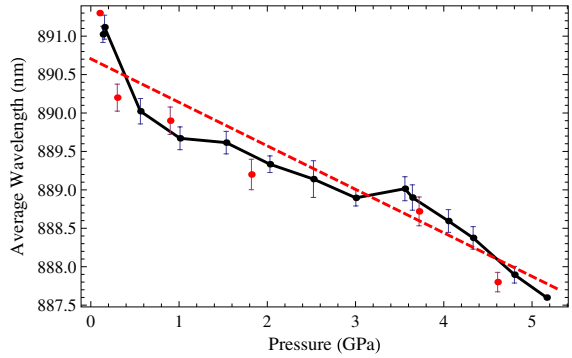

Fig. 5. Average positions of the TE and TM resonant peaks obtained using Eq. (7). Black dots show the positions of rising pressures and red dots show the decreasing pressure positions. Red dashed line is the linear fit of the rising data.

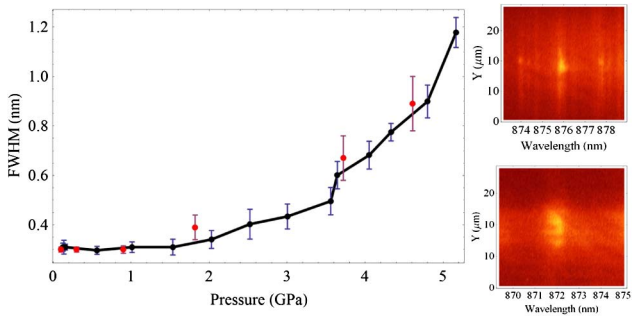

Fig. 6. Full width at half-maximum of the resonances at various pressures for the TM modes with error bars; in black the rising pressures, in red the decreasing pressures (Left). Spectral image of one resonance (Right, Top) centered about 876 nm at the lowest pressure (0.1 GPa) and (Right, Bottom) centered about 872 nm at the highest pressure (5.2 GPa).

However, this dependence must be considered as a first approximation because the mechanical elastic K property could also depend on the pressure. Moreover, if only this dependence with pressure is considered in Eq. (5), a larger shift for the average wavelength, compared to the experimental values obtained in Fig. 5, is expected.

As already mentioned, it is expected that the pressure produces an increase of the refractive index of the microspheres, and consequently, a red-shift to longer average wavelengths [see Fig. 3 (central)]. Therefore, in order to explain the experimental dependence shown in Fig. 5 (with a slope of about -0.58 nm GPa^{-1}), and taking into account Eq. (8), the dependence of the refractive index of the sphere with the pressure could be obtained from Eq. (5), i.e.,

$$\frac{\partial n_S}{n_S \partial P} = 0.0047\ \text{GPa}^{-1}, \tag{10}$$

giving rise to a dependence for the refractive index of the microsphere quite similar to those obtained in other matrices [18].

Finally, using Eq. (5) and the results obtained in Eqs. (8) and (9), a value of 6.5×10^{-4} GPa^{-1} was obtained for the average sensitivity. This value is slightly higher than 5.7×10^{-4} GPa^{-1}, which corresponds to the sensitivity of the ruby obtained using the Piermarini equation given by Eq. (1). As previously mentioned, this average sensitivity depends only on the physical properties of the microsphere itself, and it is independent of the properties of the pressure transmitting medium employed given the particular values of the inner and outer refractive index.

Another interesting parameter of the TE and TM resonances is the FWHM as a function of pressure, which is shown in Fig. 6 with black dots for increasing pressure and red dots for decreasing pressure. The limit of resolution in our experiment was 0.3 nm, and it is the value observed for FWHM up to around 1.5 GPa. At higher pressures, the FWHM had a growing behavior that can be attributed to many phenomena, but the most reasonable explanation is that it was caused by the effect produced by inhomogeneous pressure due to nonhydrostaticity of the silicone media.

First, it is important to remark that the pressure measured along the chamber by the rubies leads to a difference of about 20% at 5.3 GPa, which indicates nonhydrostaticity in the pressure chamber. This result indicates, beyond experimental errors, that the pressure is not perfectly hydrostatic in this silicone medium. It is a well known effect that the ellipticity on an optical resonator can increase the FWHM of the resonances. This ellipticity, which can be produced by elastic deformations of the sphere under inhomogeneous pressure, can induce an apparent broadening of the resonances. This is supported by the Figs. 6 (Top and Bottom), which correspond to the spectral images of the same resonance at ambient and 5 GPa, respectively; the results show that the broadening is different along the spatial axis of the image.

The abrupt point about 3.5 GPa is in good agreement with other studies on similar silicone medium that show nonhydrostaticity using the broadening of the ruby emission lines [16].

It is remarkable that although the resonances were undistinguishable at pressures above 5.3 GPa, this process is completely reversible and the FWHM decreased to its initial value of 0.3 nm when the pressure decreased to its initial value, as the red dots show.

5. CONCLUSION

The resonant WGM of Nd^{3+}-doped glass microspheres were studied as a function of pressure inside a DAC up to 5 GPa by using a silicone oil as the pressure transmitting medium. It was found through simulations that, under experimental conditions, the average wavelength of the TE and TM modes does not depend on the refractive index of the silicone oil, which makes this average wavelength a good candidate for an optical pressure sensor. Furthermore, the resonances spectral width reveals interesting behavior as a nonhydrostaticity gauge.

ACKNOWLEDGMENTS

The authors thank the Ministerio de Economía y Competitividad of Spain (MINECO) within the National Program of Materials (MAT2010-21270-C04-02), the Consolider-Ingenio 2010 Program (MALTA CSD2007-0045, www.malta-consolider.com), and the EU-FEDER for financial support. The authors also thank ACIISI of Gobierno de Canarias for project ID20100152 and MICINN for the FPI grant BES-2008-003353.

REFERENCES

1. V. K. Rai, "Temperature sensors and optical sensors," Appl. Phys. B **88**, 297–303 (2007).
2. G. Adamovsky and M. V. Ötügen, "Morphology-dependent resonances and their applications to sensing in aerospace environments," J. Aerosp. Comput. Inf. Commun. **5**, 409–424 (2008).
3. K. J. Vahala, "Optical microcavities," Nature **424**, 839–846 (2003).
4. L. L. Martín, C. Pérez-Rodríguez, P. Haro-González, and I. R. Martín, "Whispering gallery modes in a glass microsphere as a function of temperature," Opt. Express **19**, 25792–25798 (2011).
5. L. L. Martín, P. Haro-González, I. R. Martín, D. Navarro-Urrios, D. Alonso, C. Pérez-Rodríguez, D. Jaque, and N. E. Capuj, "Whispering-gallery modes in glass microspheres: optimization of pumping in a modified confocal microscope," Opt. Lett. **36**, 615–617 (2011).
6. L. L. Martin, P. Haro-González, I. R. Martín, D. Puerto, J. Solís, J. M. Cáceres, and N. E. Capuj, "Local devitrification of Dy^{3+} doped $Ba_2TiSi_2O_8$ glass by laser irradiation," Opt. Materials **33**, 186–190 (2010).
7. H. Masai, S. Tsuji, T. Fujiwara, Y. Benino, and T. Komatsu, "Structure and non-linear optical properties of $BaO–TiO_2–SiO_2$ glass containing $Ba_2TiSi_2O_8$ crystal," J. Non-Cryst. Solids **353**, 2258–2262 (2007).
8. L. L. Martin, D. Navarro-Urrios, F. Ferrarese-Lupi, C. Pérez-Rodríguez, I. R. Martín, J. Montserrat, C. Dominguez, B. Garrido, and N. Capuj, "Laser emission in Nd^{3+} doped barium–titanium–silicate microspheres under continuous and chopped wave pumping in a non-coupled pumping scheme," Laser Phys. **23**, 075801 (2013).
9. G. J. Piermarini, S. Block, J. D. Barnett, and R. A. Forman, "Calibration of pressure-dependence of R_1 ruby fluorescence line to 195 kbar," J. Appl. Phys. **46**, 2774–2780 (1975).
10. B. E. Little, J.-P. Laine, and H. Haus, "Analytic theory of coupling from tapered fibers and half-blocks into microsphere resonators," J. Lightwave Technol. **17**, 704–715 (1999).
11. S. Schiller, "Asymptotic-expansion of morphological resonance frequencies in Mie scattering," Appl. Opt. **32**, 2181–2185 (1993).
12. M. L. Gorodetsky, A. A. Savchenkov, and V. S. Ilchenko, "Ultimate Q of optical microsphere resonators," Opt. Lett. **21**, 453–455 (1996).
13. H. Wang, X. Lan, J. Huang, L. Yuan, C.-W. Kim, and H. Xiao, "Fiber pigtailed thin wall capillary coupler for excitation of microsphere WGM resonator," Opt. Express **21**, 15834–15839 (2013).
14. G. R. Elliott, D. W. Hewak, G. S. Murugan, and J. S. Wilkinson, "Chalcogenide glass microspheres; their production, characterization and potential," Opt. Express **15**, 17542–17553 (2007).
15. High Pressure Diamond Optics, Inc., www.HPDO.com.
16. S. Klotz, J.-C. Chervin, P. Munsch, and G. Le Marchand, "Hydrostatic limits of 11 pressure transmitting media," J. Phys. D **42**, 075414 (2009).
17. K. Shinozaki, T. Honma, and T. Komatsu, "Elastic properties and Vickers hardness of optically transparent glass–ceramics with fresnoite $Ba_2TiSi_2O_8$ nanocrystals," Mater. Res. Bull. **46**, 922–928 (2011).
18. R. G. Kuryaeva, "Refractive index and compressibility of the $KAlSi_3O_8$ glass at pressures up to 6.0 GPa," Glass Physics and Chemistry **37**, 243–251 (2011).